Indian Journal of History of Science, 43.3 (2008) 381-410

INVESTIGATIONS ON ANCIENT HIGH – TIN BRONZE EXCAVATED FROM LOWER BENGAL REGION OF TILPI

Prasanta K. Datta*, Pranab K. Chattopadhyay, Barnali Mandal***

(Received 11 April 2008; revised 19 January 2008)

Bengal has got a tradition of making bronzes right from the black-and-red ware levels of Pāṇḍu Rājār Dhibi, having different compositions of tin (Sn) in copper (Cu). The excavated bronzes by different archaeologists provide a paradigm shift in bronze making from low tin bronzes to high tin bronzes and super high tin bronzes in different archaeological contexts. The low tin bronze materials containing around 10% Sn in Cu are called α- bronzes. High - tin bronzes constitute 20 - 25% Sn and are designated as ($\alpha + \beta$) bronzes or simply β bronzes; while Sn in super high – tin percentage bronzes– mostly around, 30% Sn are called γ bronzes by metallurgists. Bengal traditionally produced all those bronzes in cast form, like many other ancient civilizations. Tilpi excavation produced a few β – bronzes, cast in nearly found crucibles. This paper has investigated metallurgical characterization of the materials in order to find out the technological aspect of the production process.

Key words: Bronze, Casting, Crucible, Hearth, SEM-EDX, XRD.

Introduction

Metallurgy began in Bengal - comprising both Bangladesh and West Bengal of India as early as 1500 BC in the Chalcolithic Age. The recent nomenclature of this culture is known as black-and-red ware culture by the archaeologists and which evolved after the Neolithic Age. Copper has been used from the early part of this culture and the use of alloy has also been traced from objects attributed

* Department of Metallurgical & Material Engineering, Jadavpur University, Kolkata- 700 032. India; e-mail: dokra_pkd52@yahoo.co.in.

** Centre for Archaeological Studies & Training, Eastern India, 4 Camac Street, Kolkata-700 016. India; e-mail: pranab108@rediffmail.com.

to the late phase of this period. Copper objects were manufactured by casting and by subsequent forging practices. Alloying with tin was known but the knowledge relating to its proper composition was not adequate. The analysed bronze specimens with more or less 9-11% tin belonging to this period was found in Bahiri, Bharatpur, Dihar, Mangalkot and Pāṇḍu Rājār Dhibi[1]. The α- bronze objects in this category mostly found are bangles, beads, earrings, finger rings, fish-hooks etc.

In the early historic period, the use of high tin bronze, popularly known as *kānsa* in Bengal and Bell Metal elsewhere was noted[2]. This Cu – alloy constitute 20 - 25% Sn belonging to β category of bronze is simply known as beta-bronze[3]. This bronze appears golden – white in color, after it has been quenched and polished. High tin bronze (*kānsa*) vessels of Bengal origin have been discovered at Ban-Don-Ta-Pet, Thailand[4]. The water bowls made of this material in cast form were brittle but its golden – white appearance was highly esteemed in society. High tin bronze mirrors, having over 30% Sn belonging to γ bronze have also been found at Chandraketugarh and Mahasthan[5]. Till to-day the use of *kānsār* (gong) or *kartāl* (cymbals) is continuing in the society at large.

Recently some detail studies on high tin bronze have been made on Indian context by Srinivasan[6] (2007), Pillai, Pillai and Damodaran[7] (2006), Datta, Ghosal and Misra[8] (2006), Datta and Chattopadhyay (2007 A[9]; 2007 B[10]).

1. Brief Introduction of Archaeological Investigation

The site Tilpi (22°15′N, 88°38′E) is located in the coastal District of South 24-Parganas, West Bengal, India (Fig. 1). The excavation (Fig. 1a) was simultaneously conducted in the nearby village Dhosa, near Jaynagar by the Directorate of Archaeology, Government of West Bengal in March 2006 and March 2007. The excavation revealed artifacts and structural evidences. At Dhosa, it was suggested that a *stupa* existed there during the 2nd and 1st century BC Excavations have unearthed a wealth of proof that it was once thickly populated by industrious and self-sufficient people. The unearthed furnace and few other analyzed materials are shown at Figs. 1(a) and 2.

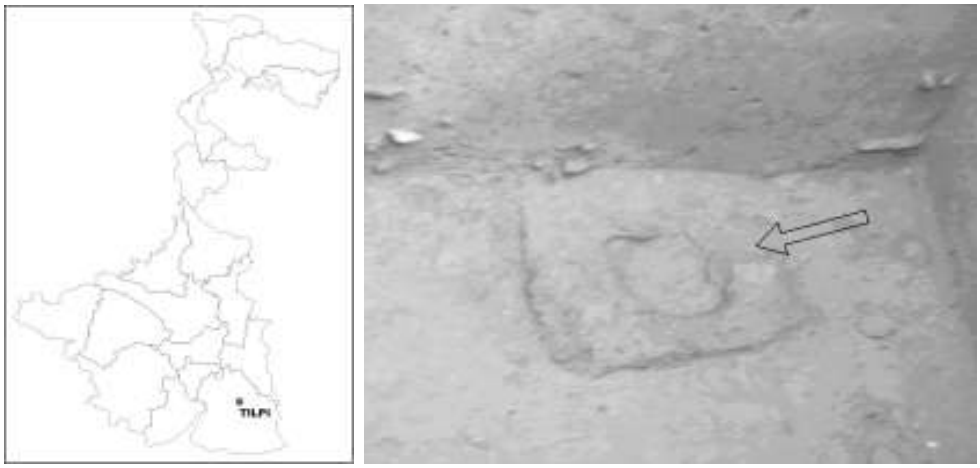

Fig. 1. Location of Tilpi , Fig. 1(a). Excavation at Tilpi, showing the formation of a hearth for metal processing, probably of non – ferrous metals like copper, bronze, brass etc. The discontinuity (right hand side) at the foundation indicates the portion of the ash- pit door, for removal of cinder. The door was also used (like *'chulas'* of sub- continental variety) for passing air blast under natural draft or forced draft, by winnowing fan, to generate heat by the combustion of fuel.

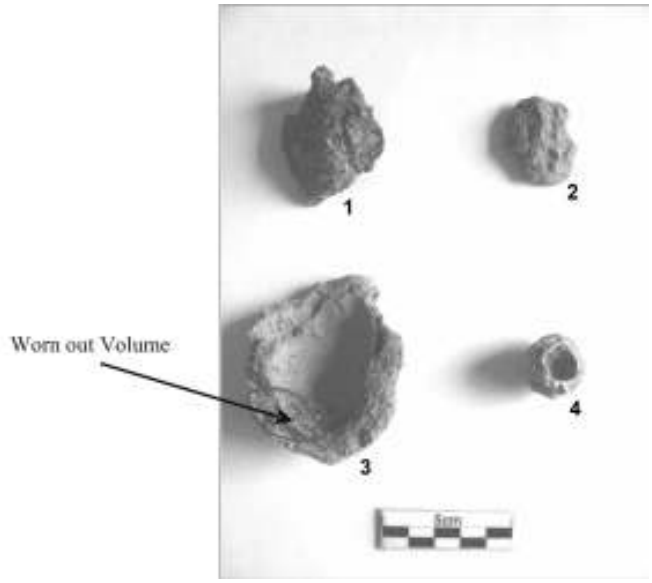

Fig. 2. Analyzed objects recovered at Tilpi, (1) Slag, (2) Metal Ingot, (3) & (4) Broken crucible fragments.

2. Identification of a Factory Site

The pieces already excavated establish the presence of the following:

i) Crucibles

ii) Slag

iii) Cast metal lump

iv) No of hearths (8 nos.)

Assemblage of the above in the same site gives enough indication of the probable presence of a factory site where metal was melted or cast.

2.1. Description of Excavated Materials

Eight hearths for smelting or melting metals have been found at this site. The excavated factory site revealed furnace remains. The foundation remains have been shown in Fig. 3.

Fig. 3. Excavation at Tilpi, showing factory site (Photograph courtesy Amal Roy). The pits presumably provide the remnants of foundation chambers for fire- place remains, or tool pockets or post - holes of working table normally operated by micro level metal workers.

2.1.1. Crucible

The size, shape and the material of the crucible fragment (Fig.4) are fascinating (Fig.5a, 5b). The outside shape resembles conics with semi-circular cross section inside, unlike modern crucibles, which are flat bottomed. From the

Fig. 4. The external surface of the crucible

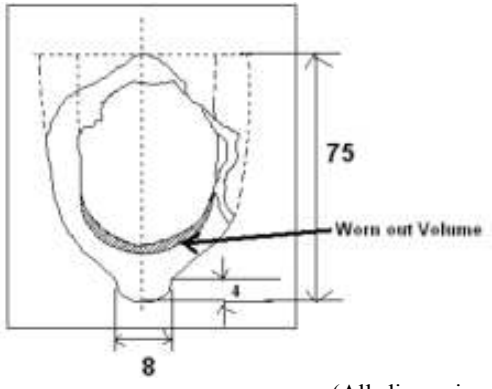

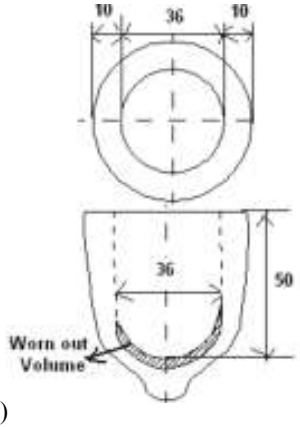

(All dimensions are in mm)

Fig. 5a. Crucible as received in excavation **Fig.5b.** Crucible reconstructed

out side shape it may be inferred that the crucible, having a pointed end at the bottom was adequately supported by solid fuels, to keep it up-right for holding liquid metal. Similar shaped crucibles were detected in contemporary Senuwar, Bihar in Kushana Period 1st-3rd century AD[11] (Singh 2004, Fig. 85, p. 375).

The material of the crucible seems to be made of fired charcoal (or graphite?) and clay. The green crucible after shaping in the die was dried and then fired slowly for achieving handling strength. The traditional practice of crucible making was probably adopted, as it is difficult to differentiate it from the modern crucible, commonly used by present day non-ferrous foundry men.

2.1.2. Reconstruction of Crucible and Metal Lump

The worn out volumes of the crucible has been masked in (3) (Fig. 2). Metal Lump (2) has got the oval bottom which matches the interior of the crucible (Fig.6).

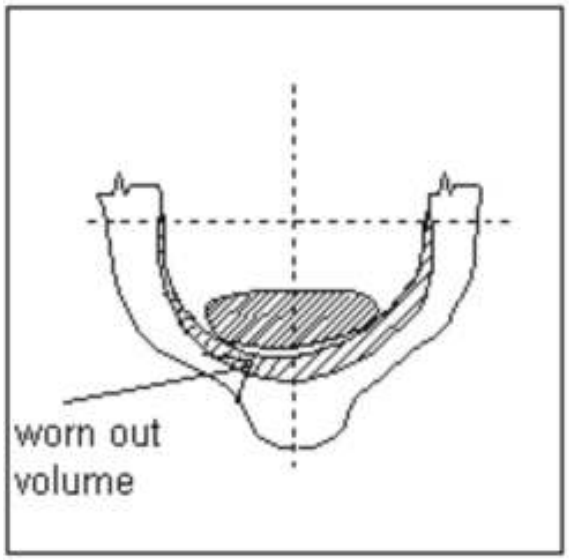

Fig. 6. Reconstructed crucible showing Lump

2.1.3. Slag

The friable object (Fig.7) found in the excavation seems a solid slag, whose chemical compositions was not determined quantitively but qualitatively the specimen contains an intimate mixture of iron – siliceous compounds.

Fig. 7. Slag specimen after brushing clay

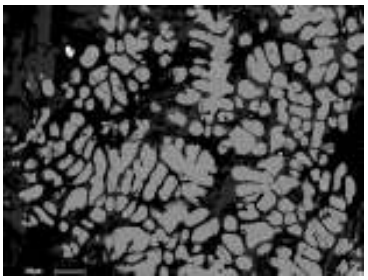

Fig. 8. Microstructure showing wustite (lighter) in analcime (dark) matrix. Wustite is FeO.

The mineralogical analyses of the slag sample was carried out through SEM and found as a combination of two phases (Fig.8). XRD of the slag specimen

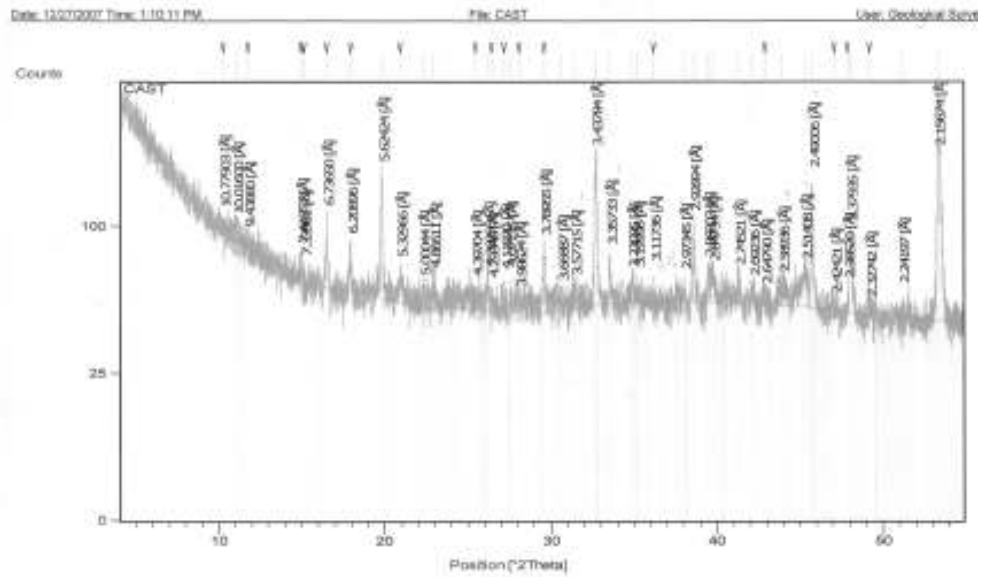

Fig. 9. 2 theta values 0 - 55° range

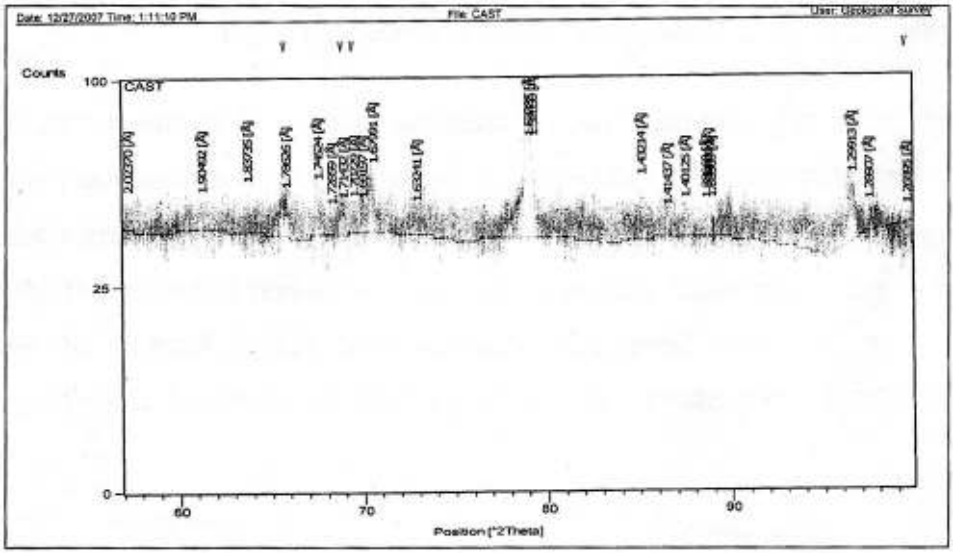

Fig. 10. 2 theta value 57-100° range

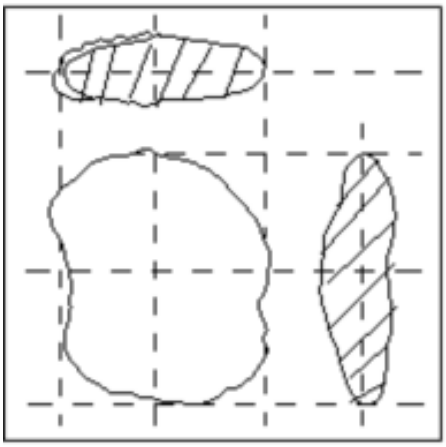

Fig. 11. Ingot sample as received in excavation

revealed analcime ($NaAlSi_2O_6$-H_2O) as major mineral phase with Wüstite (FeO) as minor one. This also include small amount of kaolinite with trace amount of ilmenorutile, mica and christobalite. The X-ray diffraction patterns are shown in Figs. 9 and 10.

3. Metallic lump at Tilpi

The copper-alloy lump (Fig. 11) discovered at this site, was coated with greenish blue hydrated copper carbonate corrosion layer, as usual like any archaeo-copper objects. After removing the clay, the lump was oval in appearance and irregular in shape but flat on top with blunt edges. It was around 35 mm x 30 mm x 8 mm in dimensions and weighed approximately 35.3242 gm. The drawing of the lump was made and shown in Fig. 11. From visual inspection and matching it seems that the copper object might have been cast in the bottom hole of the given crucible which might be subjected to some kind of cool air blast (Sea breeze or rainy wind).

Copper or tin bronze is a good corrosion resistant material, yet under buried condition, micro-organisms often colonize the surface and their masking areas, with the surrounding moist (hydrated) environment lead to bio-corrosion of the alloy. As the microbial population increases, ultimately those microbes gradually envelop the external surface, with the under side metal getting corroded. The corroded bronze specimen has been shown in Fig. 12 which can be divided as follows:

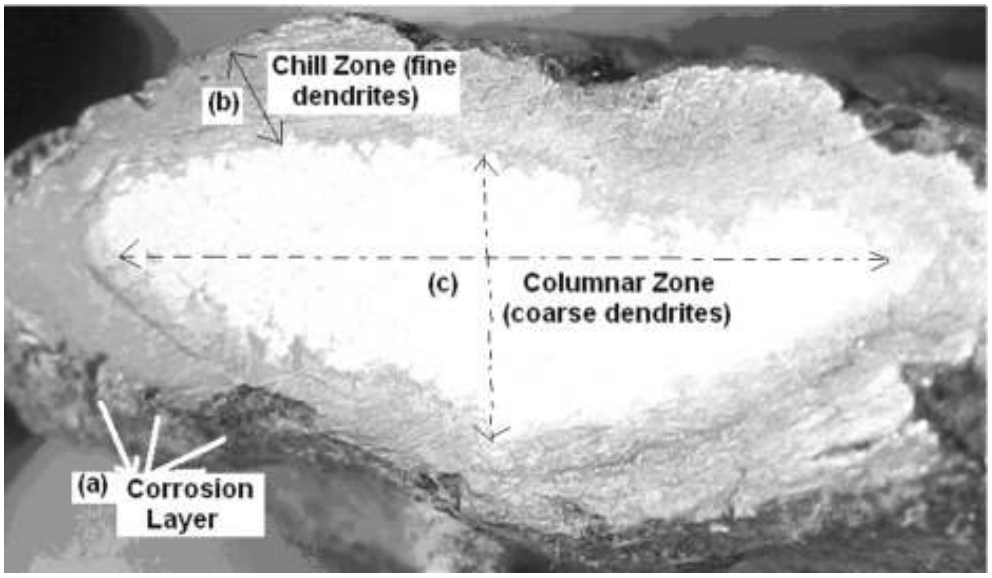

Fig. 12. The macrostructure of metallic lump. (a) The thin corrosion layer covers (black used in the picture) the surface. The chill zone and columnar zone can be clearly seen in the macrograph.

(a) Outside Corroded layer, mixture of Copper hydroxide and hydrated Copper carbonate, (b) Chilled Zone (finer grain structure) due to faster cooling, (c) Large volume of Columnar Grains (shown by dotted line) Coarse dendrites grow due to slow cooling inside.

3.1. Corroded layer of Metallic Lump

The corrosion mechanism of the bronze sample can be constructed as:

(i) **Oxygen concentration cell**[12] where the under belly of microbes covering the metal surface becomes low oxygen concentration area or cell **anode**. The open surface of metal surrounding microbes with the medium of moisture or under ground water, having high oxygen concentration areas (round the microbes) acts as cell **cathode**.

(ii) A Galvanic couple of the electrolytic cell[13] develop between low oxygen concentration area (anode) and high oxygen concentration areas (cathode), where Cu or Sn slowly oxidizes.

Anode half – cell reaction: (i) $Cu \rightarrow Cu^{++} + 2e^-$

(Oxidation) (ii) $Sn^{2+} \rightarrow Sn^{4+} + 2e^-$

Cathode half – cell reaction (Reduction):

(iii) $O_2 + 2H_2O + 4e^- \rightarrow 4OH^-$

Standard Electrode Potentials[14] at 25^0C, E^0 volts vs. Standard Hydrogen Electron (SHE) of the above reactions are,

(i) + 0.337 V , (ii) + 0.150 V, (iii) – 0.401 V

(negative sign is due to the reverse reaction shown)

Naturally either copper or tin whichever be the metal gets dissolved in (OH^-) the hydrous system, forming the corrosion product of $Cu(OH)_2$, copper hydroxide. Cu being bulk, $Cu(OH)_2$ formation will be more.

The type of corrosion can be called **Oxygen Concentration Cell** corrosion. Sometime there is a possibility of Cu – Sn galvanic couple formation, where overall reaction becomes,

$Sn^{+2} + Cu^{2+} \rightarrow Sn^{4+} \downarrow + Cu$

If the high- tin concentration phases 'β' or 'δ' (later discussed) becomes anode and the high copper concentration phase, α – phase becomes cathode. This would rather help the kinetics of corrosion occurring in microbial ecology or biogeochemistry would be strengthened. This type of corrosion is called **Galvanic Corrosion**.

The corrosion product further gets boost by the acidic carbonyl secretion of bacteria and converts Cu $(OH)_2$ to $CuCO_3$.

Cu $(OH)_2 + H_2CO_3$ (carbonyl acid) $\rightarrow Cu(OH)_2 , CO_3 \downarrow + 2H_2O$

The corrosion product has got a greenish blue color like a mixture of Azurite[15] $[Cu_3(OH)_2 (CO_3)_2]$ and Malachite $[Cu_2(OH)_2 CO_3]$ (green).

Sometime a mixture of copper – tin carbonate complex in greenish color also forms deposit over the metal surface.

3.2. Macrostructure of Metallic Lump

The chill zone and columnar zone can be clearly seen in the macrograph (Fig. 12).

Already stated three distinct zones result:

(a) Outside corrosion layer of greenish colour.

(b) About 1.4 mm thick chill zone of finer dendrites (grey).

(c) Coarse grains of columnar dendrites (white) in core.

The chill zone (grey areas), annular in shape is the second part, where due to faster cooling, fine grains of copper rich dendrites solidify first. The red hot crucible with liquid metal as soon as was taken out of the furnace, cooled very fast by the surrounding cool air at ambient temperature (Fig. 13). The quenching action moves through the crucible to chill the freezing metal at the outside boundary. So, a small chill zone of around 1.4 mm developed in the solidified ingot.

With passing of time the hot crucible got colder and the temperature gradient of the crucible with outside flattened, slowing down heat transfer rate. So, the freezing rate of liquid metal also slowed down. A coarse grain structure of columnar tin rich dendrites grew inside (shown in Fig. 12, by dotted line in white area). The slow freezing helped the nucleated crystals to grow more.

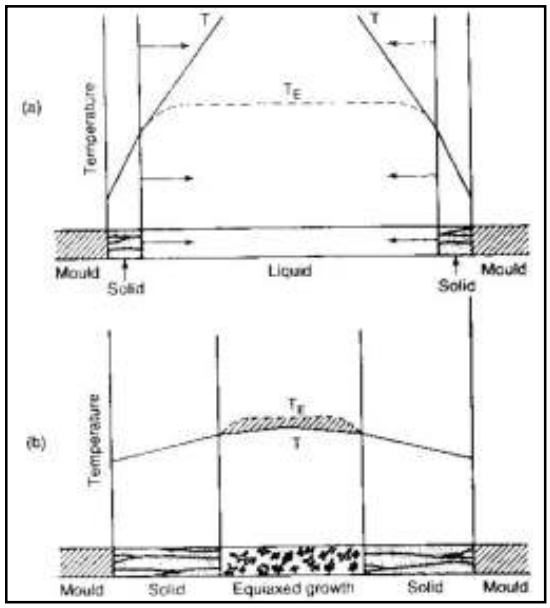

Fig. 13. Thermal explanation of mixed structures in castings. (a) Chilled zone, arrow shows freezing direction (b Collumnar and equiaxed region when temperature gradient is flattened.. (after Beeley[16]).

3.3. Chemical analysis of Metallic Lump

The composition of the metal sample as analyzed by SEM-EDX provides an elemental composition of Cu: 73.09, Sn: 24.37, Ni: 0.28, Fe: 045, S: 1.76, Si: 0.06. This infers that the metal lump comes in the group of a high-tin β - bronze alloy having a composition of ~75% Cu and 22-25% Sn alloy. It holds negligible amount of nickel, iron, sulphur and silicon as residual, from the ore.

3.4. Microstructure of Metallic Lump or Tilpi bronze

The SEM microstructure (Fig. 14) of the specimen shows the usual dendritic structure of any cast material. The dark grey phase is copper rich dendrite and the light grey phase surrounding dendrites is tin rich β -phase. Some of the primary dendrites in the central region are very coarse and grew definitely from the large solidification time available in a shutdown crucible.

3.4.1. Further Nucleation in Core of Metallic Lump

The long freezing time in core of the metallic lump allowed a convective mass transfer within the core of the freezing liquid. The convective current grows out of the buoyancy force of heavy copper (density 8940 kg/ m^3)[17] and high melting point (1356K) with respect to lighter tin (density 7280 kg/ m^3)[18] with lower melting point (505K). Convective heat transfer further under cools the remaining last-to-freeze liquid between already solidified coarse columnar dendrites. Cluster of atoms then facilitate α – phase to nucleate between coarse dendrites.

High rate of nucleation produces very fine grains because of large under cooling (ΔT) below the equilibrium liquidus temperature (T_E)[19] (Fig. 13). ΔT is designated as under cooling and defined as (T_m- T) (T_m = melting or freezing temperature of metal and T = Prevailing temperature of the metal during freezing.

This is due to the fact that the large ΔT values lowered the critical nucleus size r^* (as $r^* \alpha 1/\Delta T$)[20] down to a very small amount. Small r^* values enhance the kinetics of nucleation. There could also be directionality of heat from freezing liquid towards the mold surface (here crucible). Due to the directional solidification a kind of acicular grains or dendrites can be located in the microstructure (Fig. 14).

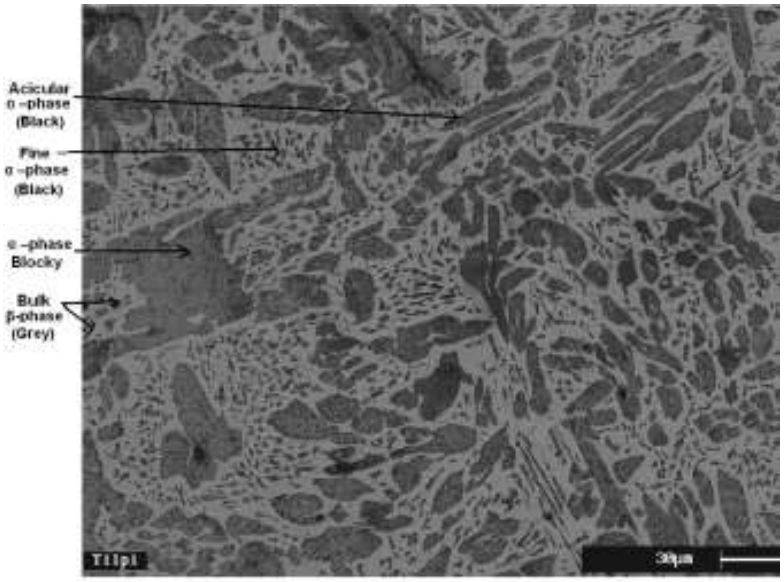

Fig. 14. Microstructure at the central region of cast ingot. Black areas represent solid solution of tin in copper, known as α –phase. Note some dendrites of α –phase look blocky and some are acicular (lens shaped). Between the dendrites a large number of fine α –grains (dendrites) are visible. The bulk phase (matrix) is held by tin-rich, solid solution of tin in copper, δ, β –phases.

3.5. Coring in Dendrites of Metallic Lump

During solidification any grain or dendrite, at first, nucleates and then grows until restriction occurs from outside. So, the first solid composition can be obtained in the center of the grain and the last solid composition would be available at the edge of the grain. For the reason above, a large grain of α -phase (marked by arrow in Fig.14) has been selected for analysis. EDX composition started from the center of the dendrite and ended at the boundary of the dendrite (Fig. 15) that is from point marked 1 (centre) to point marked 6 (at the edge). The first solid contains 13.66 wt.% Sn and the last solid at the frozen edge the tin percentage rises to 16.78 wt.% - a slow incremental progress of Sn% as prescribed in phase diagram (Fig. 17): C_S (low Sn%) $\rightarrow$ C_L (high Sn%). The results detailed the presence of Cu, Sn and Fe, which is shown in Table – 1. All these signify the phenomenon of heavy coring[21] (deviation from average chemical composition) of the primary dendrite, α-phase of Cu-Sn solid solution, in the microstructure. Naturally, like all cast bronzes the bronze structure looks heavily cored.

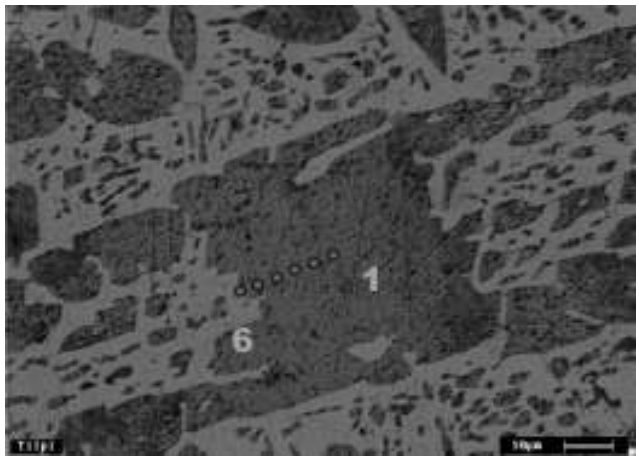

Fig. 15. A primary dendrite has been selected for micro – analysis by SEM – EDX to understand the coring characteristics. The center region represented by point [1] contains more solvent, Cu as expected and the skin represented by point [6] contains more solute, Sn as theoretically prescribed[22].

Table 1: Compositions of a primary dendrite 4µm apart

Points	Cu	Sn	Fe
1	85.24	13.66	1.10
2	84.59	14.11	1.30
3	84.94	14.03	1.03
4	83.66	15.10	1.24
5	82.17	16.97	0.86
6	81.96	16.78	1.25

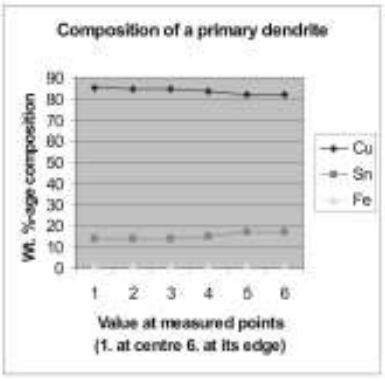

Fig. 16. Composition of a primary dendrite 4µm apart.

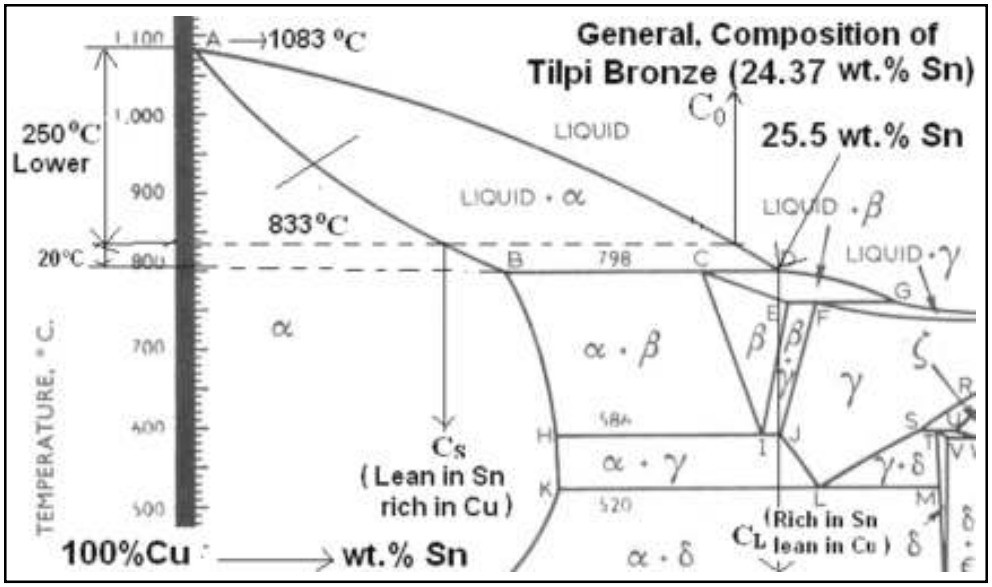

Fig. 17. A part of Cu-Sn phase diagram, showing the relevant portion[23].
C_S- 1st solid composition that froze at the center. 1st solid (low tin copper) dendrite center. The solubility of tin increase from 10 wt.% (B) to 13 wt.% (H) as shown by BH or HK line when temperature drops from 1071K (BD line) to 859K (HJ line).

3.5.1. Non-equilibrium Freezing of (Cast) Metallic Lump – Chilling Practice

Already stated, from the centre of the dendrite, tin percentage starts from 13.66 by wt. % and finishes at the edge by 16.78 wt. % at the surface as indicated by Fig.16. This coring or micro-segregation is due to the non-equilibrium freezing of the alloy during casting as expected with Cu-Sn alloy[24]. This signifies the probable knowledge of metal workers, in the long freezing range characteristics of Cu-Sn alloy family, which is unlike short freezing range alloys of Cu-Zn family. This knowledge of long freezing range characteristics encouraged the people to have as slow as possible cooling mechanism, for achieving good feeding of freezing alloy, to avoid micro-shrinkage phenomenon at the last stage (center of the ingot). But the micro shrinkage defects associated with this bronze is surprisingly very less in this metal sample. This is not incidental but likely to be intentional. Modern physical metallurgists know that with increase in tin content in copper alloy from 10% to 24%, the solidification range shrinks from ~170K to around 20K (table 2) and the short freezing range, β – bronze casting becomes easier to feed for producing sound and strong metal (later discussed). For achieving the directional

solidification, to counteract the risering problem of Cu-Sn alloy, this slow solidification was probably replaced by fast cooling of the metal β – bronze at the outside. This fast cooling or chilling practice was introduced by ancient metal workers so that the micro-porosity creation of bronze and the centerline shrinkage could be centralized.

3.5.2. The Randomness of Dendrites

The dendrites cover the micrograph in a haphazard fashion (Fig.14). This random orientation is an indication of the formation of highly super cooled region within casting, where the temperature gradient of the cooling liquid lagged the equilibrium freezing temperature curve of solute rich (tin rich) freezing alloy[24]. This region is already described in the macrograph (Fig. 12). Naturally the isotropic dendritic nature rather than, preferential directionality of grains or dendrites for the casting, occurred in the last stage of freezing.

3.5.3. Relationship of Dendritic Arm Spacing of Metallic lump

A random measurement of Secondary Dendritic Arm Spacing (DAS) was undertaken to have an idea of the cooling rate expected in the casting. The relationship between the cooling rate, (R in ^{0}C/Sec) and (λ in μm) can be determined by the following[25],

$$\lambda = 101 \times R^{-0.42} \qquad \ldots(1)$$

From the values of dendritic arm spacing, when (i) λ = 8 μm, R = 380ºC/Sec, (ii) λ = 14 μm, R = 110ºC/Sec, (iii) λ = 30 μm, R = 14ºC/Sec, and (iv) λ = 50 μm, R = 5.33ºC/Sec were calculated. Against λ = 8 μm, the cooling rate R = 380K/Sec, indicates very fast cooling rate to be obtained for quenched metal and for λ = 50 μm, the cooling rate is R = 5.33K/Sec, which indicates very slow cooling rate. Both of these are extreme freezing rates of the alloy and shows a mixture of coarse and fine dendrites coexist in the central part of the casting (Fig. 14).

3.6. Short Freezing Range of Metallic Lump as High Tin Bronze

The freezing range of 24 Sn – 76 Cu alloys (Tilpi bronze) is short, about 20 K (Fig. 17) and can be categorized as a **Short Freezing Range alloy**.

3.6.1. Short Freezing Range Alloys - Sound Casting Easier by Risering

Solidification of short freezing range alloys[26] (Fig. 18) usually start at the mold interface where heat extraction is greatest. The chilling action of the mould wall results in the formation of a thin skin of solid metal surrounding the liquid. With further extraction of heat through this shell of solid metal, the liquid begins to freeze onto it and the wall of solid increase in thickness overcoming mushy zone[27].

The solid and liquid portions are separated by a relatively sharp line of demarcation – the solidification front – which advances steadily towards the center of the casting. Short freezing range alloys encourage directional solidification even at relatively low thermal gradient.

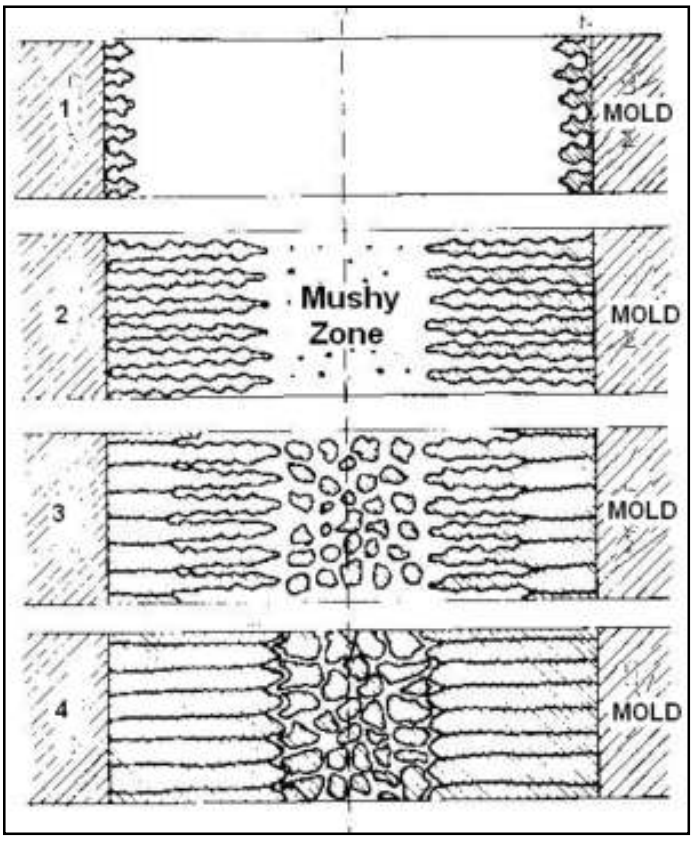

Fig. 18. Schematic mode of freezing of short freezing range alloys (after Strauss[28]): (1) Starting stage, Chill Zone (2) Columnar dendrites, (3) Central Equi-axed Zone, (4) End of freezing, Final grain structure.

From metallurgical view point, Short Freezing Range Alloys produce consistent mechanical properties like Cu-Zn alloys (Brass) or killed steel ingots. Short Freezing Range alloys solidify directionally close to plane front solidification that is the freezing surface starts from mold / metal interface and finishes at the center. Therefore, like killed steel, the total or final shrinkage or pipe concentrates at the center and by directional solidification, or risering, sound cast metal can be produced easily by feeding liquid metal at the last stage.

3.6.2. Short Freezing Range Alloys - Stronger Cast Metal

One further advantage, from technological view, accrues. The chance of micro-porosity formation diminishes and the micro-crack which is initiated from the porosity generally lacks momentum. Therefore, the working stress, σ, as per modern 'Fracture Safe' criteria[29],

$$\sigma = K_{1c} / \{A \times v (2\pi a)\} \qquad \ldots(2)$$

where 2a = Inside crack size, K_{1c} = Fracture toughness, A = Geometrical factor, does not deteriorate. (Note, bigger the crack size'2a', lower the value of σ)

3.6.3. Freezing Range – High Tin Bronze vs. Low Tin Bronze

In composition up to 10%Sn – 90%Cu alloys or low tin bronzes are long freezing alloys – freezing range vary as high as 180 K (Table 2). Tin addition to pure copper increases freezing range from 0 K– 180 K, up to 13.5 wt. % Sn – Cu bronzes.

Table 2: Freezing Range for Alloys due to Addition of Tin to Copper

Addition of wt.% Sn to Cu	0	2	6	10	11	13.5	16	18	20	22	24	25	25.5
Freezing Range Temperature(K)	0	75	140	170	175	180	152	125	100	65	35	10	0

Then, further addition of Sn to bronze, reduces Freezing Range (Fig. 19). Lower freezing range improves castability as well as soundness. The reason is that all these Long Freezing Range Alloys (low tin bronzes) solidify in random dendritic solidification[30] and produce lots of micro- porosity, which are difficult to fill or feed by risering and naturally produced unsound (inside spongy) cast metals of

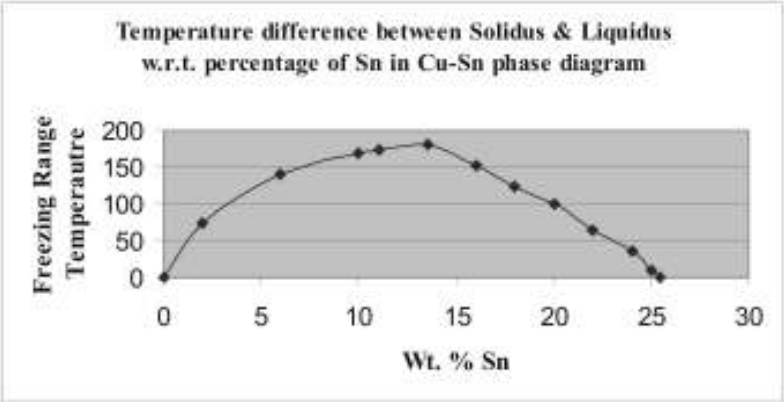

Fig. 19. Freezing Range for Cu-Sn Bronzes from 0 – 25.5 wt. %Sn.

lower, inconsistent mechanical properties. The working stress, σ comes down as the denominator in the equation (2) has large values. High tin bronzes comparatively are more sound and reliable than low tin bronzes.

The spongy[31], weak, castings of low tin bronze (10Sn90Cu alloy) were discarded in favor of short freezing, easily fed, high – tin (22 – 25%) Cu alloys. The β- bronze was favored for its sound metal, generating sharp tonal quality with consistent sonic response.

3.6.4. Short Freezing Range Alloys Produce Better Fluidity

Liquid Copper interestingly, has a viscosity[32] of 4.8 m Ns/ m^2 and tin (liquid) has 1.15 m Ns/ m^2 at their respective melting points of 1356K and 485K. The gradual increase of tin to copper physically decreases the viscosity of bronzes. As viscosity is closely related as the inverse of fluidity[33] so the addition of tin to copper surely makes the foundry property of bronzes better than pure copper, so far fluidity of liquid bronze is concerned. So, being more fluid casting production by bronzes become easier.

Simultaneously, the melting points also of Cu-Sn alloys or bronzes come down, lower than melting point of copper (Fig 17). Tilpi bronze has lower melting than Copper.

Foundry alloys like bronzes melt easily because of lower melting points. Both these properties are beneficial for foundry men and high- tin bronze making became very popular. These two advantages of castability were probably noticed

by Bengal metal workers and the casting technology of Bengal worker became much simpler proposition than working with liquid copper.

3.7. Coring in Inter - Dendritic Region of Metallic Lump

Chemical analyses of compositions for last-to-freeze liquid (Table 3) using EDX were determined. The compositions of last-to-freeze liquid metal indicate the high concentration of Sn in the last to freeze liquid alloy as expected (Fig.17) by C_L (rich in tin). The common micro-segregation phenomenon experienced elsewhere is quite apparent in the result obtained (Fig.20). As solidification comes to the last leg of solidification, there is an acute accumulation of low melting point solute Sn, in Cu. Coring, as discussed earlier during dendrite formation, also appears naturally.

Table 3: Compositions of Last-to-freeze liquid.

Cu	Sn	Fe	Ni
64.92	34.71	-	0.36
65.05	34.50	-	0.45
64.83	34.67	-	0.50
64.29	34.42	0.78	0.501
64.54	34.92	0.13	0.41
73.09	24.37	0.45	0.28

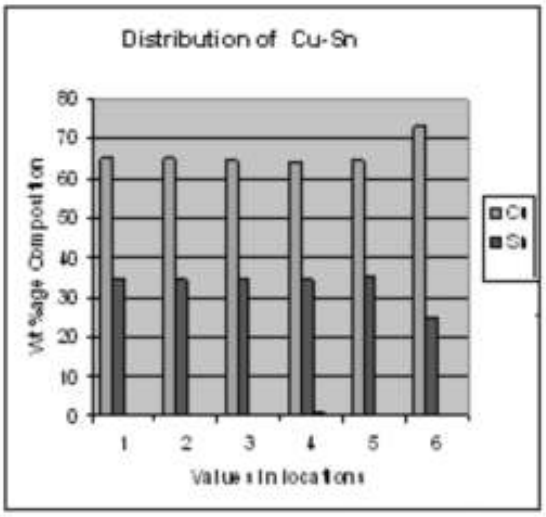

Fig. 20. Distribution of elements Cu, Sn in Last-to-freeze liquid.

3.7.1. Iron Content in Metallic Lump

Iron content is also significant, as an impurity element - starting from 1.10 wt.% at centre and it rises to 1.24 wt.%, though Fe-Sn metallic compounds can not be excluded as the reverse segregation.

The maximum solubility of tin in α – solid solution of copper, as per the Cu-Sn phase diagram 15.8 wt.% Sn, but the chemical composition of the center of the dendrite is 16.78 wt.% Sn. As Cu – Sn- Fe become ternary alloy system and the maximum solubility of Sn in Fe is 17.7 wt.% Sn (Fig. 21), therefore, in presence of iron the solubility of tin in the bronze system probably has increased.

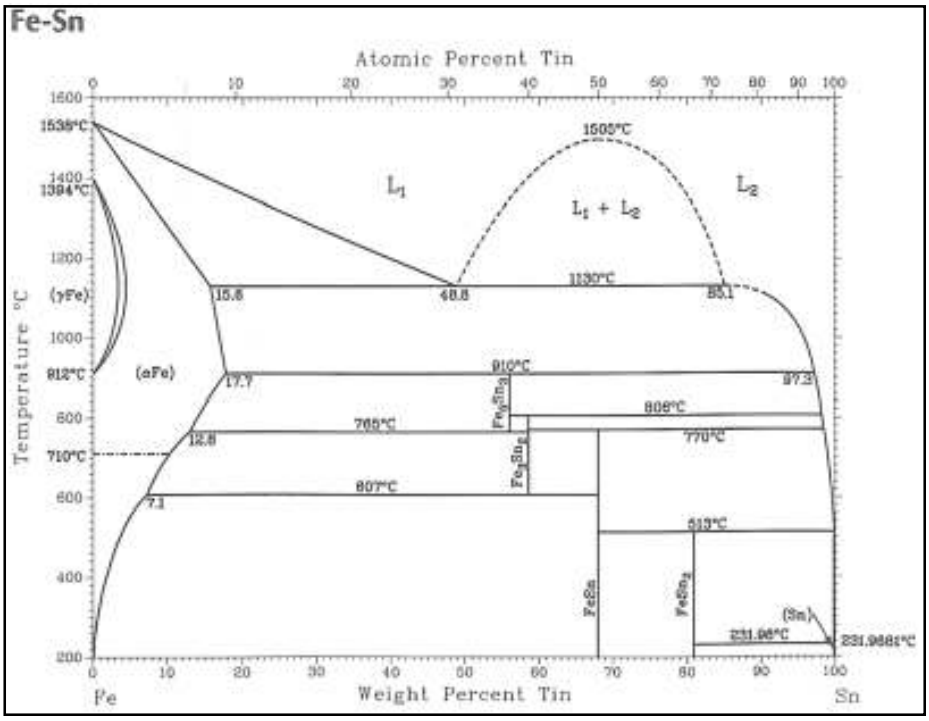

Fig. 21. Fe-Sn Phase diagram (after ASM[34]).

3.7.2. Effect of Iron in metallic lump

Iron in small amount during solidification precipitated in the as-cast structure and refines the grain by inhibiting grain growth. Presence of free iron[35, 36] produces a hardening effect (later discussed) accompanied by brittleness and loss in elongation. The hardening effect and the idea of grain fineness were probably

known to Bengal metal workers. The assumption is due to the fact that slag lumps contained lot of ferrous constituent in the given sample of Tilpi (2.1.3).

3.8. Chemical analysis of an interesting dendrite

The SEM analysis of Tilpi bronze specimen has revealed an interesting dendrite, which has heterogeneous region in the center as shown in Fig. 22. The iron- silicate compound of the core throws a new light that the addition of Cassiterite (tin ore) was probably very common in Bengal / Eastern India to isolate tin from its ore. As Cassiterite contains lot of silica, remnants of that silica might entrain the copper during bronze making. Note the high amount of tin, 66.68% in the analyzed core of the dendrite. The chemical composition of the center region of the dendrite is Fe: 3.06%, Cu: 11.90%, Sn: 66.68%, O: 16.10%, Si: 1.94%, S: 0.36%, Ni: 0.02%. The entrapped silica, probably as ceramic particles, helped as substrate to form the dendrites of this high-tin bronze alloy.

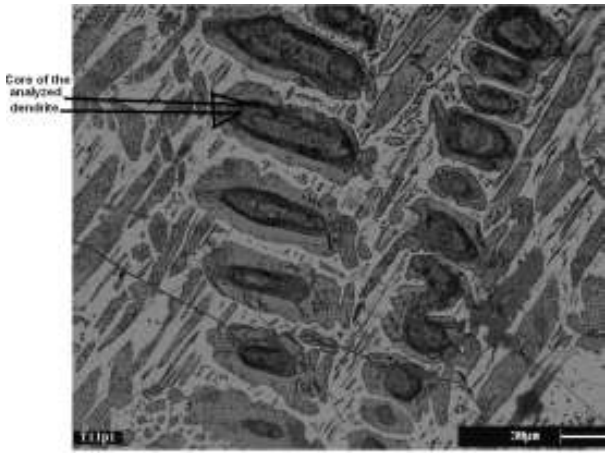

Fig. 22. The microstructure holds a special dendrite whose core or substrate looks completely different. The analysis of core revealed a iron-siliceous substrate, which acted like heterogeneous nucleants during the formation of these dendrites.

3.9. Source of Copper from Impurity Nickel, in metallic lump

Ni is also a very common impurity of Singhbhum copper as identified by Sahu[37](2004), contains Cu: 15.00 wt.%, Ni: 10.85 wt.%, Co: 0.37 wt.%, Fe: 26.6 wt.%, S: 33.3 wt.%. Considering the very low oxygen potential of Silicon for oxide formation, the use of Silica can be assumed from Si / O_2 ratio; because

the availability of oxygen in the substrate is 16.1 wt. %, which is much above the requirement as 1.94% Si requires stoichiometrically 2.2% Oxygen to form Silica.

3.10. High Strength and Hardness of metallic lump

Tin was added to copper to make it harder or stronger and the phenomenon goes by the name of solid solution hardening[38]. Soft gold, in antiquity was strengthened by either silver or copper and is still the prevalent practice to make gold stronger, suitable for jewelry making. More solute (tin) goes to the solution (copper), stronger become the alloy. This hardening technique was mastered by metal workers and the workers added almost double the amount of tin (from 10% to 24%), to get a very hard bronze, almost four times harder than pure copper. Pure Cu has 55 VPN while macro hardness of the lump determined was 228 – 231 VPN (Table 5)[39].

The above observation is vindicated by the following results:

Both micro and macro hardness of the Tilpi bronze specimen were obtained by Vickers' Micro Hardness Machine, Leica make. Micro-hardness results are shown in Table 4 taken on both over dendritic region and outside dendrite region. Table 5 also shows the Macro-Hardness results obtained through Vickers Macro Hardness Machine, Model no. HPO-250.

The micro hardness results also corroborate the non-equilibrium freezing of the alloy concerned. Uniformity in the HV values has been obtained over primary dendrites. But a scatter of HV values 188.5 to 454.2 signify the presence of hard high-tin rich phase δ or β″ or micro-shrinkage within the last-to-freeze areas.

Table 4: Vickers' Micro - Hardness (MODEL: LEICA VMHT)
Load = 15gf, Time: 20sec.

No.	Dia (d_1,μm)	Dia (d_2,μm)	Outside Dendrite (Grain) HV ($Kg.\mu m^{-2}$)
1.	7.8	7.8	454.2
2.	12.1	12.1	188.5
3.	8.7	8.8	284.0
No.	Dia (d_1,μm)	Dia (d_2,μm)	Within Dendrite (Grain) HV ($Kg.\mu m^{-2}$)
1.	8.7	8.8	362.0
2.	8.6	9.2	351.7
3.	9.3	9.0	331.0

Table 5: Vickers' Macro - Hardness (MODEL: HPO-250)

Load = 30Kg

No.	Dia (d_1,μm)	Dia (d_2,μm)	Sum ($d_{1+}d_2$) μm	Avg. Dia (d,μm)	Hardness (Kg.μm^{-2})
1.	0.491	0.497	0.988	0.494	228
2.	0.477	0.499	0.976	0.488	234
3.	0.490	0.491	0.981	0.491	231

Table 6: Identified phases from X-ray diffraction data

No	Angle θ /Ω 2.1	d_{space} Å	Rel I I/I_0	Identified Phase	Diffracting Plane (hkl)
1	26.4	3.3733	32	δ phase	110
2	26.6	3.3482	33	δ phase	012
3	28.7	3.1078	29	δ phase	020
4	29.6	3.0153	29	δ phase	–
5	33.9	2.6422	38	Sn, δ, β′ phases	110,112, 110
6	36.5	2.4596	100	Sn, δ phase	101, 022
7	37.7	2.3841	31	δ phase	120
8	42.3	2.1349	89	δ phase	113
9	42.4	2.1301	87	δ phase, β′ phase	030,111
10	43.1	2.0971	42	δ phase, α- Cu	122,111
11	49.2	1.8503	36	Sn, α- Cu, , β′ phase	032, 200,200
12	51.6	1.7699	42	α- Cu, δ phase	200,221
13	51.8	1.7634	43	δ phase	123
14	55.0	1.6681	35	δ phase	222
15	61.4	1.5087	55	δ phase	223
16	61.8	1.4999	43	Sn, δ , β′ phases	034, 112,121
17	65.8	1.41623	39	δ phase	231
18	72.1	1.3089	45	δ phase, β′ phase	232, 202
19	72.7	1.2996	46	α- Cu	220
20	73.3	1.2905	53	δ phase	016
21	73.8	1.28293	45	δ phase	233
22	77.0	1.2374	42	δ phase	044, 116
23	77.2	1.2347	43	δ phase	143, 330

Note: β′ and δ- phases are solid solutions of Sn in Cu (δ – phase = $Cu_{10}Sn_3$) and Pure Tin phase occurs from inverse segregation of tin.

The micro hardness of dendrite is slightly more than expected in virgin Cu-Sn alloy as some impurities like Fe, Ni already inhabit the system.

3.11. X-ray Diffraction (XRD) Analysis of metallic lump

Analyzing the X- ray diffraction data (Table 6) a number of phases have been identified[40]. The important phases located (Fig. 23) can be summarized as:

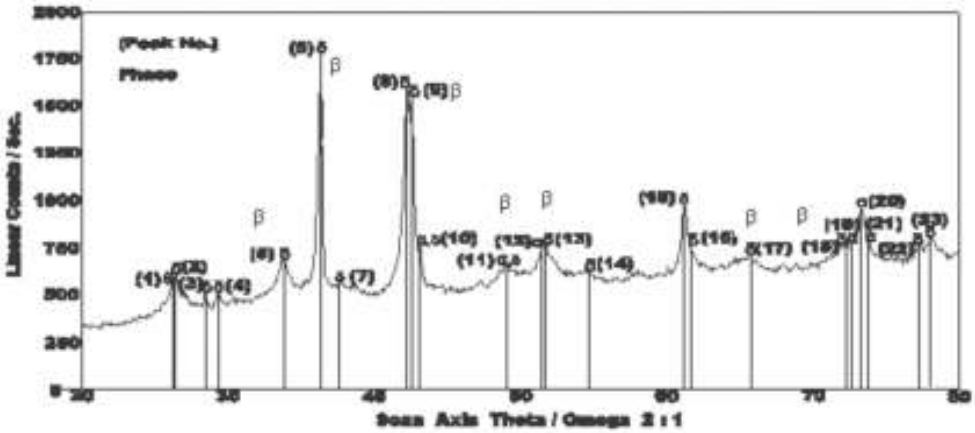

Fig. 23. XRD Pattern of the Bronze sample found at Tilpi

Pure Tin, α, β′ or β″ and δ solid solutions of Cu-Sn phases.

Pure Tin in cast copper - tin alloys during freezing squeezes out and sometimes comes outside the casting surface by means of inverse segregation ("Tin Sweat")[41]. So, a pure tin phase appears.

β′ & β″ solid solutions of copper-tin alloys are meta-stable phases, which remains untransformed during cooling.

From $\beta \rightarrow \alpha + \delta$, eutectoid transformation occurs and the reaction product, α (solid solution) is copper rich and softer phase.

δ or β′ or β″ are harder phases of copper-tin solid solution and imparts very high hardness comparable only to high-carbon steels[42].

Conclusion

The present observation has revealed many new information of Early Historic Bronze making in Eastern India. The copper is obtained from rich Singhbhum copper belt, of the Chottanagpur region in the West of Bengal. India is not rich in Tin ores, though small tin deposits of Cassiterite, are scattered over Baster – Malkangiri pegmatite belt (Pal et. al 2007)[43] of central India, several places of Hazaribagh, Ranchi, Gaya, Giridih and (Baghmundi areas) Purulia districts. Conversely in the East of Bengal (present Bangaladesh) very rich deposits of Cassiterite are available from ancient time near Indian coast line, in contiguous regions of South China, Burma, Thailand and Malay, which still supplies largest amount of tin in the world even to-day.

Sourcing both copper and tin, Bengal developed long freezing range (as high as 170 K) low- tin (<10%) α – bronzes (Cu: Sn = 9: 1) like any other civilizations elsewhere in the world. The problems of mushy zone, high micro porosity, poor fluidity with comparatively inconsistent mechanical properties and high melting point (~ 1323K) near to melting point of copper were definitely headache to copper founders or metal workers. In search of better metal of lower melting points, those workers added more tin (low melting point metal, 505K) to the alloy system in Cu: Sn = 3:1 ratio, rendering it to a short - freezing range alloy. Thus, high tin β – bronze (22 – 25% Sn-Cu alloy) eliminated many material drawbacks of earlier bronzes and added better mechanical properties, even with good sonic quality.

The production of this excellent material needed a good grasp of metallurgical knowledge and well trained technical personnel, of which the factory set – up at recently excavated Tilpi is a bright example. Tilpi excavation produced melting shop foundations along with the foundry items like graphite crucible, cast metal and slag. The graphite crucible though small, has peculiar shape, not available in modern foundries and slag contains constituents of dross mixers. Metallic lump, identified as β – bronze, was covered with thick corroded layers, probably of bio-corrosion, normally to be developed in submerged estuary environment. The metallurgical investigation revealed the microstructures of the bronze sample which clearly established that the manufactured item is a piece of casting. SEM – EDX analysis further identified the respective phases, contained by the alloy which can be compared to any quality metal of the modern time. X-ray diffraction technique vindicated the micro- structural analysis. Without the help of modern metallurgical knowledge of phase diagrams and physical metallurgical laboratory, the ancient metal workers produced such a quality β – bronze, which any modern metallurgical shop would love to imitate.

ACKNOWLEDGEMENTS

The authors thank Dr. Gautam Sengupta and Shri Amal Ray of the Directorate of Archaeology, Government of West Bengal, who have given opportunity to study the excavated materials of Tilpi. The Paleontology Department of the Geological Survey of India, Kolkata has extended SEM-EPMA support. We specially thank Shri Sabyasachi Shome for his analytical approach.

NOMENCLATURE

A : Geometrical factor

Cu : Copper

C_0 : Average composition of the metal

C_S : Composition of the metal in solid stage

C_L : Composition of the metal in liquid stage

E^0 : Standard Electrode Potential, volt

Fe : Iron

K_{1c} : Fracture Toughness in Critical intensity factor in plain strain mode

Ni : Nickel

O : Oxygen

R : Cooling rate

S : Sulphur

Si : Silicon

Sn : Tin

T : Temperature in Kelvin, degree C + 273.

T_m : Freezing/ Melting point of the metal, Kelvin

T_E : Equilibrium liquidus temperature of the metal

Zn : Zinc

2a : Inside Crack Size (Crack inside the metal)

e : Electron

r^* : Critical nucleus size

λ : Dendritic Arm Spacing

δ : Working stress

ΔT : Super cooling (T_m- T) where
T is Temperature of the liquid metal

References

1. P.K Chattopadhyay, *Archaeometallurgy in India: Studies on technoculture in early Copper and Iron Ages in Bihar, Jharkhand and West Bengal*, K.P. Jayaswal Research Institute, Patna 2004.
2. D. Hanson and W.T. Pell-Walpole, *Chill Cast Tin Bronzes*, Edward Arnold & Company, London 1951; R.F. Tylecote, *A History of Metallurgy*, 1st ed., The Metal Society, London, 1976; M. Goodway and H.C. Conklin, *Archeomaterials*, Vol.2 (1), 1987, pp. 1-27.
3. M.B. Cortie and C.E. Mavrocordatos, "The decomposition of the beta phase in the copper-tin system", *Metallurgical Transactions A*, 22A, (1991) 11-18.
4. W. Rajpitak and Neigel J. Seeley, "The bronze bowls from Ban Don Ta Phet, Thailand: an enigma of prehistoric metallurgy", *World Archaeology* 11.1 (1979) 26-31.
5. P.K. Chattopadhyay, "Metal finds from Chandraketugarh, West Bengal: Archaeotechnical studies", in G. Sengupta and S. Panja, ed. *Archaeology of Eastern India: New Perspectives*, CAST, Kolkata 2002, pp. 451-61.
6. Sharada Srinivasan, "Megalithic high-tin bronze: Ethnoarchaeological and Archaeometallurgical insights on manufacture and possible artistic and musical significance", *Man and Environment*, 31.2 (2006) 1-8.
7. R.M Pillai, S. G. K. Pillai and A.D. Damodaran, "Shaping of bronze of Ancient India – some case studies from South India", *Transaction Indian Institute of Metals*, 59.6 (2006) 847 – 864.
8. P. K. Datta, S. Ghosal and D. Misra, Material Characterization of Ancient High- Tin Bronze, in *First Afro-Asian Conference on Advanced Materials Science and Technology*, (AMSAT 06) Seminar proceedings, 2006, Cairo, Egypt., pp. 244-256.
9. P.K. Datta., P.K. Chattopadhyay and A. Ray, "New evidence for high-tin bronze in Ancient Bengal", *SAS Bulletin* 30.2 (2007) 13-16.
10. P.K. Datta and P.K.Chattopadhyay, "Superior Copper Metallurgy of Eastern India and Bangladesh in medieval period: From pure copper to high-tin bronzes", *Journal of the Asiatic Society of Bangladesh* (Hum.), Dhaka, Vol.52.1 (2007) 39-55.
11. B.P. Singh, *Early Farming Communities of the Kaimur*, in Vol. 2, Jaipur 2004.
12. William F. Smith, *Foundation of Material Science and Engineering*, MeGraw – Hill Int. Edited 1993, 2nd Edition, p. 667.
13. Smith 1993, as ref. 12, p. 663.
14. Smith 1993, as ref. 12, p. 657.
15. E.G. West, *Copper and its alloys*, Ellis Horwood Series – John Wiley & Sons 1982, p. 39.

16. P. Beeley, *Foundry Technology*, Butterworth – Heinemann, Oxford, 2nd Ed., 2001, p.74.

17. *Smithells Metals Reference Book* 8th edition, edited by W.F. Gale & T.C. Totemeier, Butterworth – Heinemann an imprint of Elsevier, 2004. Vol.14, p. 19.

18. Gale and Totemeier 2004, as ref. 17, Vol. 14. p. 30.

19. P. Beeley 2001, as ref. 16, p.75.

20. P. Haasen, Physical Metallurgy, 3rd Ed., Cambridge University Press, Cambridge, 1997, p.58.

21. Paul G. Shewmon, Material Science and Engineering Series: *Transformation in Metals*, McGraw – Hill Book Company, New York, 1969, p.168.

22. P.K. Datta, "Copper and Copper alloys in Archaeological Perspective", in *Science in Archaeology and Archaeomaterials*, New Delhi, D.K. Printworld, 1995, pp. 207-270.

23. West, 1982, as ref. 15, p.107.

24. Datta 1995, as ref. 22.

25. J.D. Hwang, B.J. Li, W.S. Hwang, C.T. Hu, "Comparison of Phosphor Bronze Metal Sheet Produced by Twin Roll Casting and Horizontal Continuous Casting", *Journal of Material Engineering and Performance*, 7 (1998) 495-503.

26. J. Meredith, "Feeding of Non Ferrous alloys", *Metal – Casting and Surface Finishing* (Jan- Feb.1995) 11.

27. Sylvia, *Cast Metal Technology*, Addison Wesley Lakeville Mass., 1972, pp. 135-152.

28. K., Strauss, *Applied Science in Tin Casting of Metals*, Pergamon Press, Oxford, New York, 1st ed., 1970, p.429.

29. George E. and Dieter, *Mechanical Metallurgy*, McGraw-Hill Book Company, London, 1988.

30. Sylvia 1972, as ref. 27.

31. Sylvia 1972, as ref. 27, p.142.

32. West, 1982, as ref. 15, p.15.

33. G.H. Geiger and D.R. Poivier, *Transport Phenomena in Metallurgy*, Addison Wesley Pub. Co. Massachusetts, 1971, pp. 16-18.

34. ASM Metal Handbook, Alloy Phase Diagrams, American Society for Metals, 1992, Vol: 3, p. 203.

35. West, 1982, as ref. 15.

36. A.K. Ray, "*The production of small leaded gun-metal and leaded tin bronze castings in a small foundry"* paper presented in Symposium "Copper Alloy Foundry Practice", Transactions of a Symposium Calcutta February 1969, p.54.

37. S.K. Sahu, A. Agarwala, B.D. Pandey and V. Kumar, "Recovery of Cu- Ni and Co from the leach liquor of sulfide concentrate by solvent extraction", *Mining Engineering,* 17 (2004) 949-951.

38. Dieter 1988, as ref. 28.

39. West. 1982, as ref. 15, p.137.

40. JCPDS (Joint Committee for Powdered Diffraction System) file, 1978, *Selected powdered diffraction data for metal and alloys*, Volumes- I and II.

41. Strauss 1970, as ref. 27, p.219.

42. William F. Smith 1993, as ref. 12.

43. D.C. Pal, B. Mishra and H.J. Bernhardt,"Mineralogy and geochemistry of pegmatite hosted Sn-,Ta-,Nb-, and Zr-Hf- bearing minerals from the southeastern part of the Bastar – Malkangiri pegmatite belt, Central India", *Ore Geology Reviews Elsevier* 30 (2007) 30-55.